EARTH SURFACE PROCESSES AND LANDFORMS
Earth Surf. Process. Landforms **37**, 422–433 (2012)

Published online 1 December 2011 in Wiley Online Library
(wileyonlinelibrary.com) DOI: 10.1002/esp.2259

A progression of induration in Medusae Fossae Formation transverse aeolian ridges: evidence for ancient aeolian bedforms and extensive reworking

Laura Kerber* and James W. Head
Department of Geological Sciences, Brown University, Providence, RI 02912, USA

Received 1 April 2011; Revised 26 September 2011; Accepted 31 October 2011

*Correspondence to: L. Kerber, Department of Geological Sciences, Brown University, 324 Brook Street, Box 1846, Providence, RI 02912, USA. E-mail: Laura_Kerber@brown.edu

ESPL
Earth Surface Processes and Landforms

ABSTRACT: A progression of induration, erosion, and redeposition of transverse and networked transverse aeolian ridges (TARs) has been documented in the Medusae Fossae Formation (MFF), Mars. Cratered and eroded aeolian bedforms are rarely observed on Mars, indicating that those found in the MFF have been inactive for much longer than those found elsewhere. Indurated TARs are observed to grade into faceted MFF terrain, indicating a genetic relationship between the two. We propose that TAR deposition, induration and erosion have played a larger role in the surface morphology and evolution of the MFF than previously recognized. The deposition, induration, and erosion of TARs indicate that the MFF has undergone multiple cycles of reworking, and that much of its current surface morphology does not reflect the circumstances of its primary emplacement. Copyright © 2011 John Wiley & Sons, Ltd.

KEYWORDS: Mars; aeolian; ancient; Medusae Fossae Formation; transverse aeolian ridge

Introduction

The Medusae Fossae Formation

The Medusae Fossae Formation (MFF), is a fine-grained, friable unit of uncertain origin located near the equator of Mars (130–230°E and 12°S–12°N), which has been intensively modified by aeolian processes (Ward, 1979; Scott and Tanaka, 1986; Greeley and Guest, 1987; Bradley *et al.*, 2002; Mandt *et al.*, 2008; Zimbelman and Griffin, 2010; Figure 1). The MFF is an extremely rough deposit (on the scale of centimeters up to tens of kilometers; Kreslavsky and Head, 2000; Carter *et al.*, 2009), with heavily eroded surfaces often covered with fields of streamlined, sculpted ridges known as yardangs (Ward, 1979) (Figure 2). The MFF has been divided into three units, upper (Amu), middle (Amm) and lower (Aml), based on the color of the units and their states of degradation (Scott and Tanaka, 1986; Greeley and Guest, 1987). The lowest member is the most eroded unit and the upper member is the least eroded unit. A large number of hypotheses have been advanced to explain the genesis of the MFF, including emplacement by pyroclastic flows or ash fall (Scott and Tanaka, 1982, 1986; Bradley *et al.*, 2002; Hynek *et al.*, 2003; Mandt *et al.*, 2007, 2008; Kerber and Head, 2010; Kerber *et al.*, 2011), accumulation of aeolian debris (Scott and Tanaka, 1986; Greeley and Guest, 1987; Tanaka, 2000), paleopolar deposits formed during polar wandering (Schultz and Lutz, 1988; Schultz, 2002), or obliquity-driven deposition of ice and dust (Head and Kreslavsky, 2004).

A detailed analysis of formation hypotheses was undertaken by Zimbelman *et al.*, 1997 and Mandt *et al.*, 2008, who came to the conclusion that ash fall, pyroclastic flows, and aeolian deposition were the most likely formation mechanisms based on morphology and radar properties. Specifically, the morphology and topography of the MFF deposits was found to be dissimilar to the current polar layered deposits (Bradley *et al.*, 2002), and SHARAD radar returned no evidence of polar-like layering within the deposit (Carter, 2009). High resolution images revealed bidirectional sets of yardangs, which were interpreted to reflect jointing in the deposit, a trait that is often found in terrestrial ignimbrites (Bradley *et al.*, 2002).

The MFF has traditionally been mapped as an Amazonian deposit (Scott and Tanaka, 1986; Greeley and Guest, 1987; Werner, 2006) on the basis of low crater-size-density derived ages and several stratigraphic contacts where MFF material overlies young Amazonian lavas. The Amazonian is the youngest of the three eras on Mars, dating from between 3.4 and 2.0 Ga to the present (Hartmann and Neukum, 2001). Schultz and Lutz (1988) argued that the formation was much older based on the presence of many degraded and modified craters, which implied that craters were being continually erased, eroded, and buried by aeolian processes, and that the age determined from the superposed crater population reflected a modification age rather than a formation age. Recent work (Kerber and Head, 2010) has confirmed the findings of Schultz and Lutz (1988) regarding the erosion of craters in the MFF, and has demonstrated that based on directly observed and implied stratigraphic relations between Hesperian lava flows and outcroppings of the MFF, deposition began at the latest in the Hesperian. Kerber and Head (2010) showed that in some cases (such as the southeastern fan of Apollinaris Patera), Hesperian

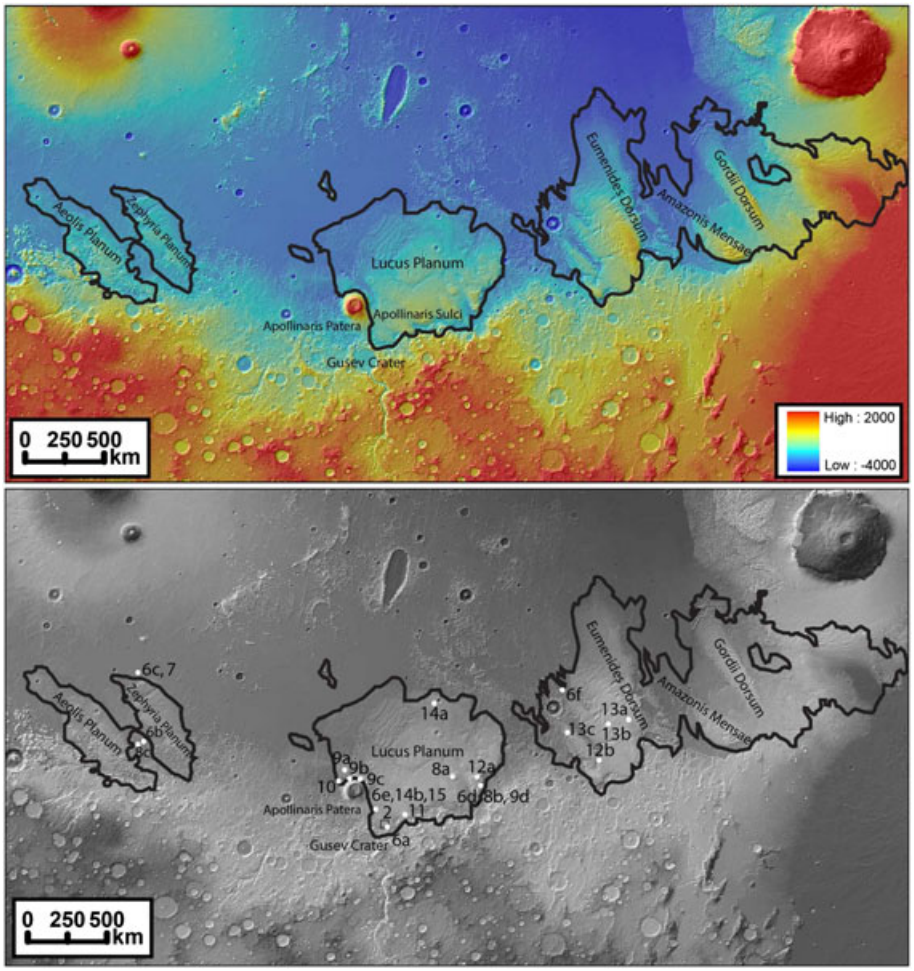

Figure 1. A regional MOLA hillshade of the Medusae Fossae Formation, stretched to show detail within the formation. Bottom panel shows the locations of the figures. Black outline indicates the boundary of the Medusae Fossae Formation as mapped by Scott and Tanaka (1986) and Greeley and Guest (1987). This figure is available in colour online at wileyonlinelibrary.com/journal/espl

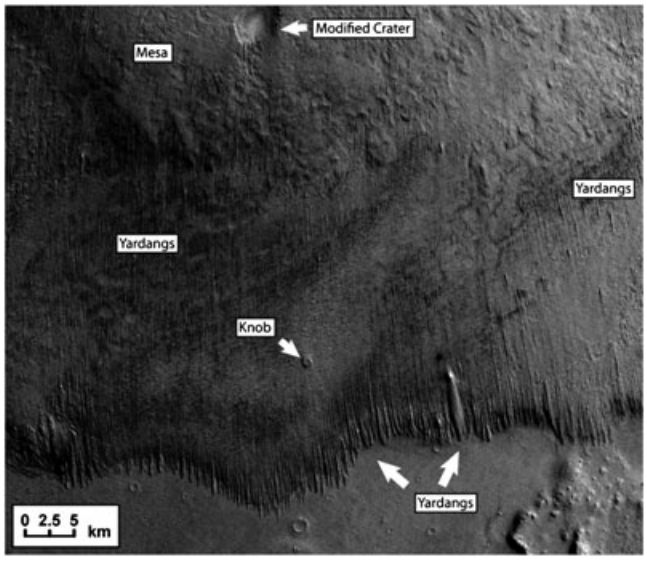

Figure 2. The Medusae Fossae Formation in Apollinaris Sulci. The formation is characterized by yardangs, mesas, knobs, and other erosional features. A portion of HRSC image h0335_0000.nd2.07.02, approximately −12.3 S, 177.3 E (Figure 1).

units directly embay the formation, burying yardangs and filling inter-yardang troughs. In other cases, Hesperian lava flows terminate in jagged, saw-tooth margins, interpreted to form when the lavas embayed the jagged edges of MFF yardangs. Once the lava cooled, the friable MFF continued to erode away, leaving a 'cast' of the MFF yardangs preserved in the lava margin. The presence of interpreted yardang 'casts' in lava margins can be used as an indicator that the MFF was present at the time that the lava was flowing across the surface in the Hesperian (Kerber and Head, 2010).

The ubiquity of yardangs and other etched and grooved terrains has led to the conclusion that most of the surfaces in the MFF are dominated by erosive processes. Tanaka (2000) suggested that given the extensive erosion present in the MFF, a corresponding volume of loose material should be present within or around the MFF as sand seas (ergs). The lack of these ergs was cited as evidence that the deposit was dominated by dust-sized particles which could be eroded and then carried to great distances. Zimbelman and Griffin (2010) estimated the heights of MFF yardangs using shadow measurements and used these heights to estimate the amount of material that would have to have been removed in order to form them. From this calculation these authors determined that some 19 000 km^3 of MFF material had been removed across the lower member of the deposit. Given the already large volume of the MFF (estimated at ~1.4 million cubic kilometers), the addition of thousands of cubic kilometers of missing mass would place important constraints on any potential formation mechanism.

In this contribution we focus on the fate of the material that is eroded from the MFF, following fine-grained eroded material from its genesis from the MFF substrate, observing how it

collects into aeolian bedforms, and then determining how the bedforms change as they age. We find evidence for locally-derived depositional aeolian bedforms made from MFF material, and come to the conclusion that depositional bedforms contribute substantially to the observed surface morphology of the MFF. We find evidence to suggest that much of the material eroded from the MFF could still be present, and that the mass that appears to be missing (Zimbelman and Griffin, 2010) may instead be locally redistributed. We begin by defining several important aeolian landforms found in the MFF in the context of those found more broadly distributed on Mars as a basis for more in-depth discussions of their morphologies.

Dunes and transverse aeolian ridges (TARs) on Mars

Aeolian erosion and transport is known to be an important geomorphological process on Mars (Greeley *et al.*, 1992). Depositional aeolian bedforms on Mars are often divided into two categories: large, long-wavelength (hundreds of meters) low-albedo dunes (Figure 3), and shorter-wavelength (tens of meters), high or intermediate albedo features known as 'transverse aeolian ridges' or TARs (Bourke *et al.*, 2003; Wilson and Zimbelman, 2004; Balme *et al.*, 2008; Berman *et al.*, 2011) (Figure 4). Large, dark dunes are commonly found in the southern hemisphere, where they have collected on crater floors, and in the northern latitudes of Mars, where they have collected into a large sand sea (erg) around the pole (Hayward *et al.*, 2007). Many different dune-types have been documented, including dome, barchan, transverse, linear, and star dunes (Hayward *et al.*, 2007). Several examples of dark dunes are shown in Figure 3. Recent work on dark dunes has shown that some dunes are active today (Fenton, 2006; Bourke *et al.*, 2008; Silvestro *et al.*, 2010; Bridges *et al.*, 2011; Geissler *et al.*, 2011). However, the majority of dark Martian dunes that have been observed over time have shown no evidence of growth or translation (Edgett and Malin, 2000; Bourke *et al.*, 2008).

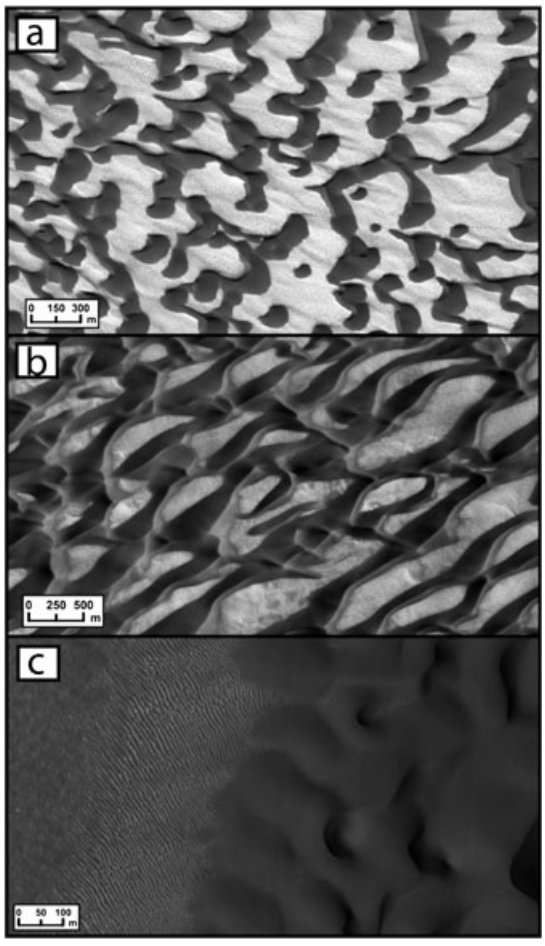

Figure 3. Large, dark dunes: (a) barchan dunes; (b) complex dunes; (c) large dark dunes (right) interacting with tranverse aeolian ridges (left). TARs usually have a much smaller wavelength compared to dark dunes. Dark dunes tend to overlie TARs where the two are observed together. Portions of HiRISE images PSP_008968_2656, PSP_010071_2615 and PSP_010077_2520, respectively.

The term 'transverse aeolian ridge', or 'TAR' was first used by Bourke *et al.* (2003) to describe small, light-toned aeolian features observed Mars, although the features had been observed as early as 1979 by Ward, who referred to them as 'transverse wind forms' (Figure 4(a)). The shorter wavelength of TARs (tens of meters) means that the feature could either be a large ripple or a small dune. Because of this ambiguity, 'transverse aeolian ridge' was used (Bourke *et al.*, 2003) as a neutral term. TARs are usually triangular in cross-section, and include a variety of diverse morphologies, including forked transverse aeolian ridges (Figure 4(a)), 'network' TARs (Figure 4 (b)), and triangular, blunt, 'barchan-like' TARs (Figure 4(c)), among others (Bourke *et al.*, 2003; Balme *et al.*, 2008). Network TARs are polygonal networks of aeolian bedforms with pointed crests which often occur in the bottoms of craters, probably as a result of multiple dominant wind directions. TARs of different types can sometimes grade into each other depending on the regional topography and wind regime; Figure 4(d) shows an example of networked TARs grading into linear TARs.

TARs are often similar in morphology to terrestrial coarse-grained ripples (Ward, 1979; Wilson and Zimbelman, 2004; Zimbelman, 2010; Zimbelman and Griffin, 2010; Berman *et al.*, 2011). Terrestrial coarse-grained ripples are characterized by a core of fine sand coated with surfaces dominated by coarse sand or gravel (>1 mm) (Sharp, 1963). The dimensions and wavelengths of terrestrial coarse-grained ripples are related to the grain size: larger ripples are composed of coarser particles than small ripples. The Mars Exploration Rover (MER) Opportunity drove across a field of small, light-colored TAR-like features in Meridiani Planum, finding them to be similar to terrestrial coarse-grained ripples, with poorly-sorted interior particles armored with coarser particles (Squyres *et al.*, 2004; Balme *et al.*, 2008). The Spirit rover also encountered coarse-grained ripples, finding them to be crusted and dust-covered but showing no obvious signs of erosion (Sullivan *et al.*, 2008).

TARs are even less mobile than dark dunes, almost always appearing stratigraphically below the large, low-albedo dunes where they occur together (Balme *et al.*, 2008) (Figure 3(c)). Often it appears as if the larger dunes have traveled across the TARs without disturbing their morphologies, indicating that TARs are less mobile than sand dunes, or indurated in some way (Balme *et al.*, 2008; Berman *et al.*, 2011).

Despite their lack of movement over observed timescales, however, most Martian dunes and TARs appear fresh and uneroded, with sharp dune-crests and well-defined second and third-order bedforms (Bridges *et al.*, 2007; Figure 4). Only a few martian dune fields appear to be old enough to have accumulated craters or other indications of degradation and erosion (Thomas *et al.*, 1999; Edgett and Malin, 2000; Fenton and Hayward, 2010). According to cratering statistics, most Martian dunes and TARs should thus have been active within tens to thousands of years before the present (Thomas *et al.*, 1999), yet most of them are not observed to have moved in the present epoch (Zimbelman *et al.*, 2009).

Medusae Fossae Formation TARs are often seen between yardangs, at the bottoms of craters, and at the contacts between the MFF and adjacent units. They were first recognized by

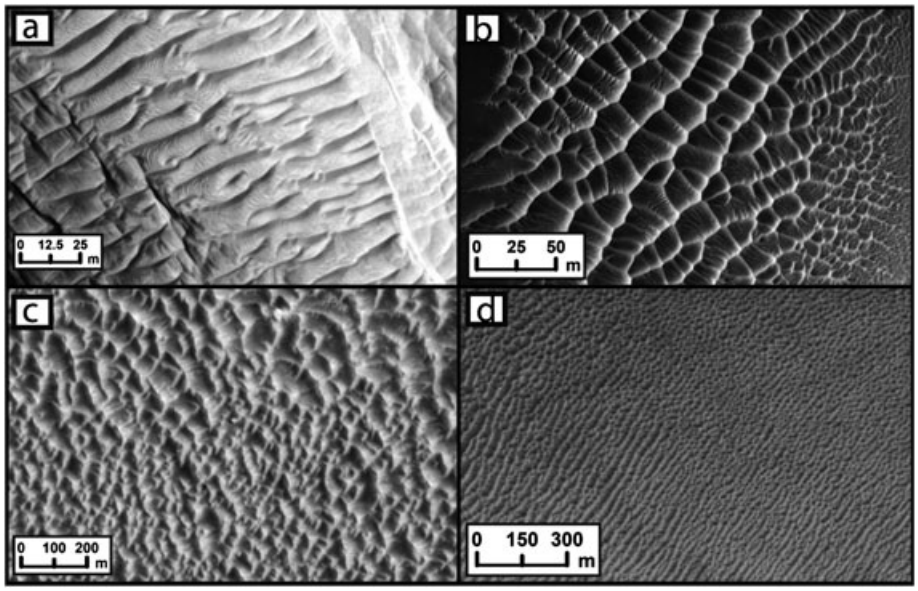

Figure 4. Typical transverse aeolian ridges. (a) Linear, forked TARs. Note sharp ridge crests and crisp secondary bedforms (bright, linear features aligned perpendicular to ridge crests). (b) Networked TARs at the bottom of Victoria Crater. Sharp crests and crisp secondary bedforms are also apparent here. (c) Type example of 'barchan-like' TARs, as identified by Balme *et al*. (2008). (d) Example of networked TARs grading into linear TARs, featured in Balme *et al*. (2008). Portions of HiRISE images (a) PSP_006879_1915 and (b) ESP_011765_1780, and MOC images (c) M1800277 and (d) R0902119.

Ward (1979), who observed that sediment formed transverse wind forms between MFF yardangs and hypothesized that they could be coarse-grained ripples, in analogy to coarse-grained ripples which are often seen in inter-yardang troughs on Earth. TARs found in the equatorial region of Mars appear to be most numerous in close proximity to fine-grained layered deposits, suggesting that these deposits may represent a source for TAR-forming material (Berman *et al*., 2011)

Yardangs

Yardangs are wind-sculpted erosional ridges that occur in deserts on the Earth and Mars (Hedin, 1903; Ward, 1979; Figures 5 and 6). They are always oriented sub-parallel to prevailing winds, with a blunt head facing upwind and a long, aerodynamically tapered tail pointing downwind (Ward and Greeley, 1984). The shape of an individual yardang has often been compared to the inverted hull of a ship, leading groups of yardangs to become known as 'fleets' (Bosworth, 1922).

Yardangs appear to be formed through a combination of aeolian abrasion (bombardment with saltating, sand-sized particles) and deflation (the plucking of grains by the wind) (Ward and Greeley, 1984). Abrasion is thought to be important at the headward end of the yardang, especially in places where the head is undercut at the height of most intense saltation, and in the valleys between yardangs, which are slowly broadened and deepened over time (Ward, 1979; Breed *et al*., 1989). Deflation appears to be important in maintaining the aerodynamic tail of the yardang (Breed *et al*., 1989). Fluting and vortex pits are often observed on the flanks of terrestrial yardangs, indicating that fine sediment suspended in complex, turbulent flows can also play a role in yardang erosion (Whitney, 1983, 1985). These flutes can be anywhere from 5 to 60 cm wide and up to several meters long (Breed *et al*., 1989).

On Earth, yardangs form at several scales and in a variety of substrates, including sandstones, siltstones, heavily eroded crystalline basement rocks, and ignimbrites (McCauley *et al*., 1977). Several fleets of a larger form of terrestrial yardang, termed 'mega-yardangs' are shown in Figure 5 (Goudie, 2007). Yardangs up to 60–80 m in height with rounded heads are found in the Lut Desert of Iran, carved into silty clays and gypsiferous sands (Goudie, 2007; Figure 5(a)). The morphology of these yardangs is modified by periodic rains which incise gullies into the flanks of the yardangs. Yardangs in the Borkou region of Chad are among the largest on Earth (up to a kilometer across) (Goudie, 2007; Figure 5(b)). These yardangs are eroded into highly lithified sandstones (Livingstone and Warren, 1996). Yardangs of the Peruvian coastal desert are carved into horizontally bedded siltstone, creating yardangs with obvious layering (Bosworth, 1922; Figure 5(c)). The morphology of an individual yardang is affected by its lithology, the availability of sand-sized particles to cause erosion, the local wind regime, and the presence of non-aeolian processes such as rain.

Martian yardangs are generally larger than yardangs on Earth (which can be meters across), but are similar in dimension to terrestrial mega-yardangs (hundreds of meters to a kilometer across) (Figure 5). Like mega-yardangs, Martian yardangs also tend to be longer in the direction parallel to the wind, up to tens of kilometers. They are found dominantly within the MFF, although yardangs are also present in the Arabia Terra region of Mars and in several outlying friable deposits (Malin and Edgett, 2000). Here we discuss only yardangs found in the MFF; these display many diverse morphologies (Figure 6).

The yardangs in the Apollinaris Sulci region of the MFF have smooth, bulbous, concave heads (Figure 6(a)). They are similar in size and shape to the Borkou yardangs (Figure 5(b)), although Martian yardangs are commonly more pointed on their upwind sides than terrestrial yardangs, which usually have rounded heads (Figure 5). In the Zephyria region of the western MFF the yardangs are more equant in shape (Figure 6(b)). These yardangs approach the 'ideal' width-to-length ratio of 1:4 needed to minimize the force of drag over the body (as documented by Ward and Greeley, 1984). These yardangs have what is called a 'keel': a medial ridge that resembles the keel of a boat. Laboratory studies have indicated that a layered substrate with a hard layer overlying a soft layer can lead to the development of keels (McCauley *et al*., 1977, 1979), perhaps indicating that some of the western MFF yardangs once had a

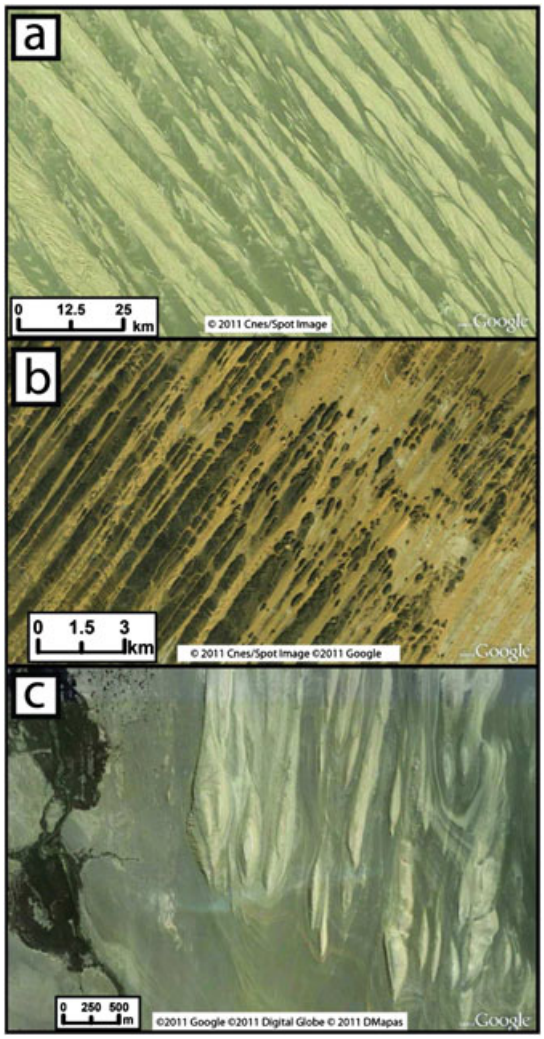

Figure 5. Terrestrial yardangs. (a) Yardangs up to 60–80 m in height in the Lut region of Iran, carved into indurated silty clays and gypsiferous sands (Goudie, 2007). A portion of SPOT 5 image from Google Earth, taken 12/03/10. lat: 30.71º N, lon: 58.26º E. (b) Mega-yardangs in the Borkou region of Chad, which cut into highly lithified sandstones (Livingstone and Warren, 1996). A portion of SPOT 4 image accessed through Google Earth, taken 12/05/10. lat: 18.80 N, lon: 19.33 E. c) Yardangs of the Peruvian coastal desert, carved into horizontally bedded siltstone (Bosworth, 1922). SPOT 5 image from Google Earth, taken 03/28/11. lat: 14.57 S, 75.60 W. This figure is available in colour online at wileyonlinelibrary.com/journal/espl

capping rock, as suggested by Zimbelman and Griffin (2010). Simple TARs can be seen between the yardangs (Figure 6(b)).

In northern Zephyria Planum, at the edge of the MFF, there occur flat-topped yardangs with a multitude of flat faces, or facets (Figure 6(c)). 'Faceted' yardangs were described by Zimbelman and Griffin (2010) in the eastern MFF (Figure 1). The facets were compared by Zimbelman and Griffin (2010) with similar features (at much smaller scales) found on ventifacts, which are caused by secondary complex flow. Similar erosion and fluting has been documented on yardangs, as discussed above, but on a much smaller relative scale to the yardang, and usually characterized by flutes that are elongated in the direction of wind-flow (Breed *et al.*, 1989). Faceted yardangs are surrounded and occasionally buried by TARs. Additional faceted yardangs with concave backs and more gently-sloping sides can be found in far eastern Amazonis Sulci (Figure 6(d)). TARs accumulate in the inter-yardang troughs.

Yardangs in western Apollinaris Sulci (Figure 1), at the foot of Apollinaris Patera (Figure 6(e)), are cut into a substrate with swirling, discontinous layers. Unlike the yardangs in the horizontally bedded Pisco formation in Peru (Figure 5(b)), the layers in Apollinaris Sulci do not appear to dip at a consistent angle, and were probably not originally horizontally emplaced.

Further to the east in the MFF, small, faceted yardangs known as 'bidirectional' yardangs are observed (Bradley *et al.*, 2002; Mandt *et al.*, 2008) (Figure 6(f)). Bidirectional yardangs are much smaller than other martian yardangs. They tend to curve around topography, and can be found in patches as well as large fields. These features are often found in thin layers overlying older, unmodified terrain. Bidirectional yardangs are not observed on Earth; their presence in the MFF is attributed to funneling of wind by pre-existing bidirectional joint sets (Bradley *et al.*, 2002).

Sakimoto *et al.* (1999) documented several generations of yardangs in the MFF, sometimes superposed on one another, which these authors interpreted as an indication of several periods of yardang formation under evolving surface winds.

While both yardangs and TARs are often long, linear features, yardangs are usually easily distinguished from TARs (compare Figure 4 and Figures 5, 6). First, yardangs are cut into the bedrock while TARs lie on top of bedrock or other sediment. Secondly, yardangs are generally much larger than TARs (hundreds of meters to kilometers versus meters to tens of meters). Third, yardangs are oriented parallel to dominant winds, while TARs are normal to wind directions; thus yardangs are often perpendicular to TARs where the two landforms occur together.

Survey and Observations

A comprehensive survey was conducted of all 270 High Resolution Imaging Science Experiment (HiRISE; McEwen *et al.*, 2007) images available as of December, 2010, that included a portion of the MFF. This was done in order to characterize depositional bedforms such as TARs and how they relate to yardangs and other MFF surface features. Mars Orbiter Camera (MOC; Malin *et al.*, 1998), Context Imager (CTX; Malin *et al.*, 2007) and High Resolution Stereo Camera (HSRC; Neukum and Jaumann, 2004) images were consulted in areas where HiRISE images were not available. It was observed that light-toned TARs are common in the formation, appearing between yardangs, on plains, and at the edges of the deposit. MFF TARs appear to be directly derived from eroding MFF yardangs, as shown in Figure 7, where MFF yardangs in northern Zephyria Planum can be seen eroding into loose material, which is organized by the wind into TARs. We can be confident that the MFF is the source of sediment for these TARs because they are cut off from alternative sediment supply sources by a vast, pristine lava plain. The accumulation of the TARs on the surface close to outlying yardangs suggests that not all of the MFF is made up of dust, which can be carried to great distances by the wind. The conclusion that the MFF is the source for this fine-grained material is consistent with the hypothesis that TARs are essentially coarse-grained granule ripples (Ward, 1979; Zimbelman and Griffin, 2010), as coarse-grained ripples are covered by >1 mm grains (Squyres *et al.*, 2004), which would be expected to be found in close proximity to their sources.

While morphologically fresh TARs are common in the MFF, many appear to be moderately indurated (Figure 8). Fresh TARs are distinguished by an albedo higher than or similar to their surroundings, sharp crests, sharp secondary bedforms, smooth, uncratered surfaces, and an absence of fluting or grooves (Figure 3). Nearly all TARs elsewhere on the Martian surface are morphologically fresh, as described above. Indurated TARs identified here are characterized by rounded, broken, or etched

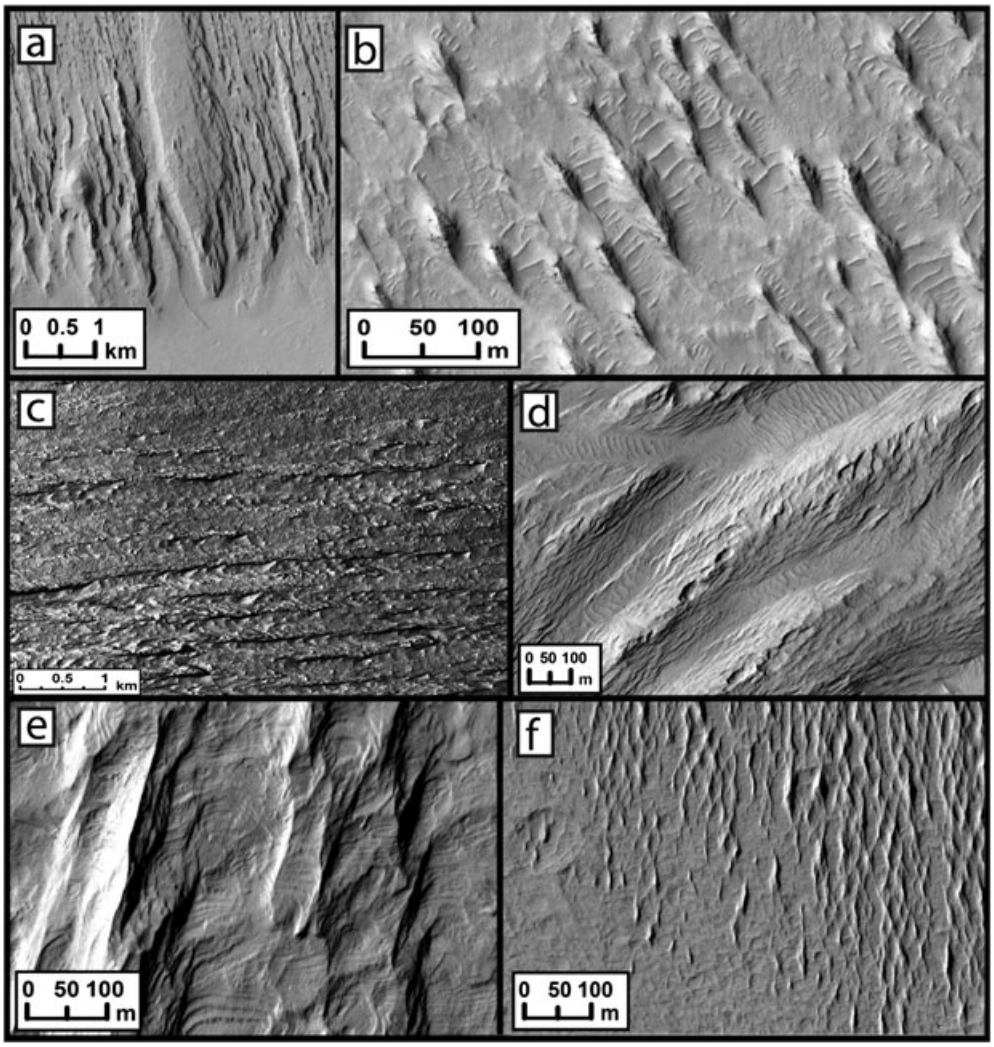

Figure 6. Yardang morphologies found in the Medusae Fossae Formation. (a) Yardangs in Apollinaris Sulci with smooth, bulbous, concave heads (portion of HiRISE image ESP_016123_1675). (b) Shorter, more equant yardangs of the Zephyria region in the western Medusae Fossae (portion of HiRISE image ESP_017047_1770). (c) Faceted, flat-topped yardangs in northern Zephyria Planum (portion of CTX image P02_001791_1852). (d) Faceted yardangs with concave backs and more gently-sloping sides, located in far eastern Lucus Planum (portion of HiRISE image PSP_006273_1715). (e) Yardangs in western Apollinaris Sulci, at the foot of Apollinaris Patera (portion of HiRISE image PSP_009464_1695). (f) Faceted/bidirectional yardangs south of Nicholson Crater. (portion of HiRISE image PSP_008158_1825). Locations are shown in Figure 1.

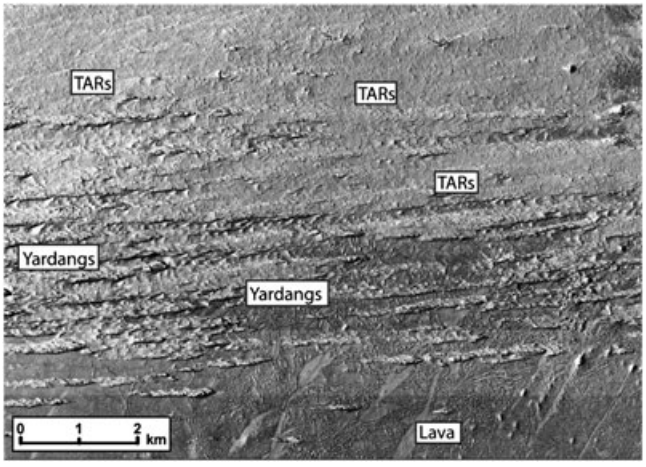

Figure 7. Fresh TARs composed of material shed by yardangs in northern Zephyria Planum (portion of CTX image P02_001791_1852).

crests, dull linear or polygonal secondary bedforms, and the appearance of superposed craters (Figure 8(a), (b)). Heavily indurated and eroded TARs are also found within the MFF, with rounded, etched, or flattened crests, rough or featureless inter-TAR areas, and a greater abundance of craters (visible at MOC-scale) than indurated TARs (Figure 9). While TARs elsewhere on Mars are generally crisp and uncratered (Thomas *et al.*, 1999), the MFF features display a distinct progression of induration from extremely fresh forms with sharp crests to dulled, abraded and eroded forms.

Figure 10 shows an area of the MFF where the progression of TARs from fresh to heavily eroded can be seen in a small geographic area. This section of the MFF is composed of a generally smooth surface marked by numerous secondaries from a nearby 22-km impact crater to the southwest. At high resolution it can be seen that there are transverse aeolian ridges (TARs) on the surface, many of which are highly eroded. Fresh-looking network TARs with crisp crests can be observed in the deeper craters (Figure 10, A), where they were either more recently active or better sheltered from erosion. Moderately degraded TARs with flattened crests and subdued morphology can be seen in slightly shallower craters (Figure 10, B), and heavily degraded TARs are present on the upper flat surface of the deposit, with fluted and crenulated crests and craters (Figure 10, D). The rays of a fresh, primary crater preserved some of the original TAR texture (Figure 10, C, dotted outline), providing evidence that the sparse bedforms that cover the surface were once more continuous, and perhaps more like an undulating sheet than a series of

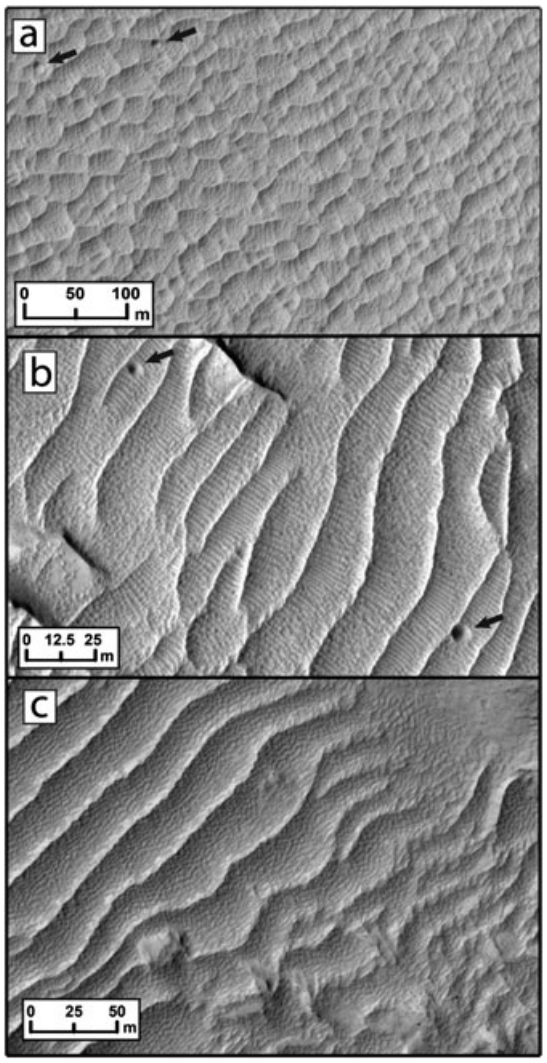

Figure 8. Indurated TARs. (a) Networked TARs of Southern Lucus Planum with subdued crests, degraded, knobby secondary bedforms, and small craters (arrows) (portion of HiRISE image PSP_008844_1730). (b) Linear TARs with flattened, crenulated crests and degraded, knobby secondary bedforms, also lightly cratered (arrows) (portion of HiRISE image PSP_006273_1715). (c) Linear TARs in a more advanced state of erosion with rounded crests, grading into complex terrain where TAR crests are flattened and interrupted (portion of HiRISE image PSP_009399_1760).

distinct ridges. This progression suggests that TARs made of similar material can experience different levels of induration or erosion based on local topographic microenvironments.

Based on the above progression, it is clear that TARs can become indurated over time, at which point they are susceptible to erosion rather than continued lateral migration as bedforms. The morphologies that result, however, can change depending on the original morphologies of the TARs, and on how exposed the indurated TARs are to the wind. For example, exposed ridges with an originally tranverse orientation can develop yardangs parallel to the dominant wind direction as they are eroded.

In Figure 11, a patch of relatively fresh network TARs (black arrow) can be seen near a small, exposed yardang which we interpret to be its source. However, this patch of network TARs sits on a rough, polygonal terrain (white arrow) with features of the same wavelength and similar morphology as the fresh network TARs, suggesting that these too were once active network TARs before becoming indurated. The superposition of fresh TARs upon indurated TARs (regardless of their source) demonstrates the evolving nature of the surface, and suggests that the landscape could, in places, be composed of layers of TARs that have undergone varying degrees of induration.

Figure 12(a) shows linear and network TARs adjacent to and continuous with the faceted terrain described above, a texture seen on and between many yardangs throughout the MFF. The close, gradational relationship between the network TARs and the faceted terrain and the identical wavelength of the polygonal patterning shared by the two feature types suggests that the polygonal 'faceting' may actually represent an indurated form of network TARs that have been subsequently dulled and modified by erosion. The origin of this faceted terrain as network and linear TARs would explain why some yardangs have smooth, flat tops, but faceted troughs and flanks: TARs preferentially accumulate in low-lying areas (Figure 12(a)). In Figure 12(b), somewhat complex, blunt, linear TARs (similar to those seen in Figure 4(c)) are clearly resolved towards the northwest part of the frame, but towards the southeast they become indistinguishable from what might be called 'complex', 'faceted' or even 'bidirectional yardang' terrain, the morphology of which might at first be assumed to be dominated by erosion. In this way, the process of TAR induration and erosion may provide an explanation for why bidirectional yardangs are so different from other Martian yardang types, as described above and shown in Figure 6. Like accumulations of TARs, bidirectional yardangs curve around topography, they usually appear to be deposited on top of the terrain instead of carved into it, and they are found in patches and topographic lows. These observations are more consistent with descriptions of TARs than with descriptions of yardangs. An origin of bidirectional yardangs from TARs would explain these similarities, and would also explain why these yardangs are different from other MFF yardangs in size and morphology. This formation mechanism would make pervasive jointing of the formation unnecessary (Bradley *et al.*, 2002), although it would not preclude the existence of joints.

Possible end-members of this induration process for both network and linear TARs are shown in Figure 13. The different starting morphologies of TARs can explain why the faceted terrain observed in different areas would show linear or polygonal patterns. Changes in TAR wavelength, as would be expected in topographic hollows, would be mirrored in the final faceted surface, as seen in Figure 13(a). This state would not be the end-state for these features, however. Instead, as wind passed over the complex features, etching and winnowing would begin to dominate, with the locations of resultant notches and flutes controlled by the repeating topography of the indurated TARs. An intermediate terrain can be seen in Figure 13(c). This image shows a field of features interpreted to be heavily indurated network TARs with notches and grooves eroded into their former crests. Eventually the original TARs will become difficult to recognize, leaving only a highly grooved and notched terrain that resembles a jointed surface. In this manner, terrain dominated by indurated bedforms of one orientation can be eroded into yardangs of a different orientation, or in the case of network TARs, bidirectional yardangs (Figure 14(a)).

The induration of bedforms and the deposition of new bedforms on top of indurated forms could eventually lead to the formation of a type of aeolianite (a rock formed from sediment that was deposited by the wind and subsequently lithfied; Sayles, 1931). We use the term 'aeolianite' as an alternative to 'sandstone' in order to focus on the mode of deposition (by the wind) rather than the grain size; however aeolianites have the same broad-scale morphological characteristics as sandstones (Sayles, 1931). Swirling, discontinous layers are commonly found in terrestrial aeolianites as a result of the deposition of successive layers and the subsequent planing of their complex surface morphologies (Kocurek, 1991).

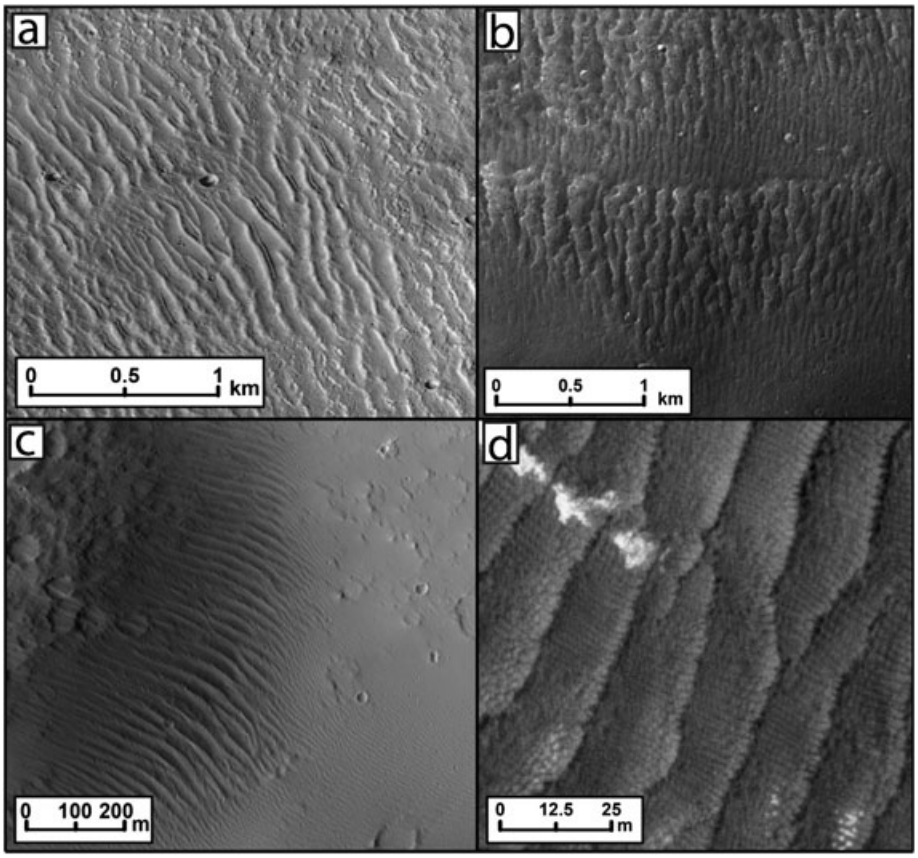

Figure 9. Heavily eroded, etched, and cratered TARs in Lucus Planum. (a) TARs north of Apollinaris Patera. Note rounded crests, subdued topography, etching, and superposed craters (portion of MOC image M1301069). (b) Eroded TARs with flattened crests. Smaller, secondary bedforms at the edges of the field are also eroded and cratered (portion of MOC image M1003186). (c) Indurated TARs sheltered by a nearby hill display rough, crenulated crests (portion of HiRISE image PSP_002634_1725). (d) Eroded dunes in eastern Lucus Planum are heavily eroded and modified, with rough and discontinuous crests (portion of HiRISE image PSP_006273_1715).

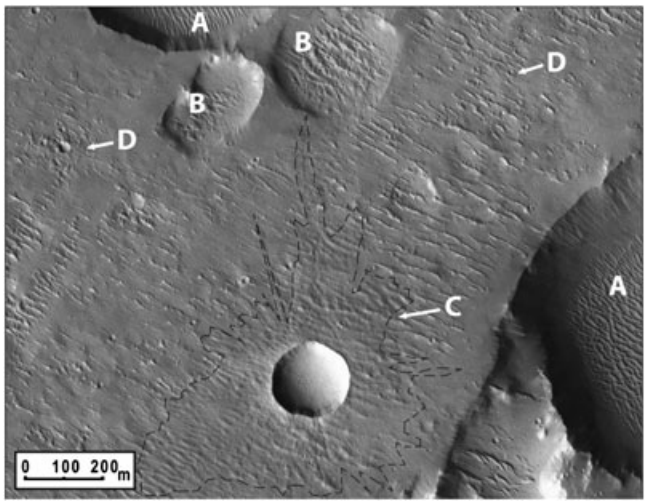

Figure 10. A region of the Medusae Fossae Formation northeast of Apollinaris Patera showing the progression of TARs from fresh to highly eroded in one image. A Relatively fresh-looking TARs with sharp crests are preserved in the deeper craters. B Slightly more degraded TARs fill the shallower craters. C The rays from a fresh primary crater (dashed line) have preserved the morphology of nearby TARs. TARs covered in ejecta have remained full and undulating, while elsewhere on the surface the TARs have been eroded into slightly sinuous remnant ridges. D Small impact craters are superposed on the remnant TARs. Portion of HiRISE image PSP_003966_1725.

Aeolianites made from layers of superposed TARs might lack fine-scale cross-bedding, but they would still develop complex and variably dipping bedding as a result of the layering of undulating, indurated forms. Erosion of an aeolianite could explain the swirling, discontinuous layers seen in yardangs in Apollinaris Sulci (Figure 14(b)). The yardangs in this area are heavily jointed, but their joint orientations do not seem to affect the orientation of the yardangs. Terrestrial aeolianites such as the Navajo Sandstone are also pervasively jointed (Hodgson, 1961). Figure 15 compares an outcrop of the Navajo Sandstone to a yardang of the MFF. Both faces have jointing on similar scales and subtle layering. While other processes can result in these kinds of layers (namely ignimbrite emplacement), this kind of morphology could also result from reworking.

Discussion

Fresh TARs exist in the MFF region, but their abundance and volume appears to be much less than the volume of material that seems to have been removed from the deposit by erosion (Zimbelman and Griffin, 2010). We have documented a wide variety of aeolian bedforms that appear to be indurated and undergoing erosion. On the basis of these observations, we propose that aeolian bedforms created as a result of erosion from the MFF can be rapidly indurated and degraded, and thus that a large number of the 'eroded' surfaces present in the formation may have previously been depositional surfaces. If this hypothesis is correct, then much of the 'missing' volume of the MFF may actually still be present in an extensively reworked form.

In order for dunes to be preserved in the eroded state seen in the MFF, they must have been subject to some kind of

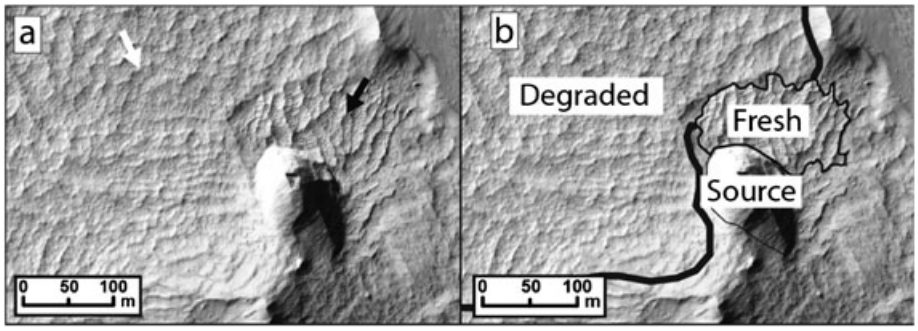

Figure 11. The transition from recognizable aeolian bedforms to degraded terrain. (a) A patch of fresh aeolian material (black arrow), interpreted to be eroding from the knob at center right, is superposed on older, indurated bedforms with subdued crests (white arrow) (Portion of HiRISE image PSP_009398_1685). (b) A sketch map outlining the units discussed in (a).

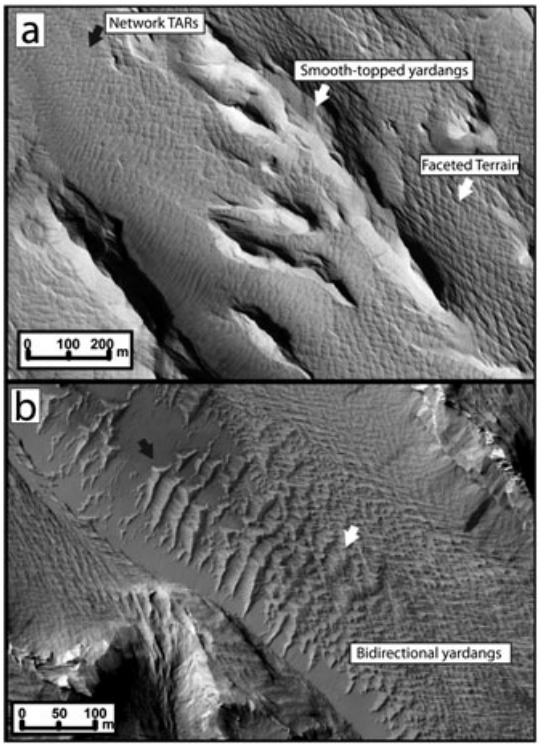

Figure 12. (a) Network and linear TARs (black arrow) are often seen in association with 'facets' with an identical pattern and wavelength (lower white arrow). In this case smooth-topped yardangs are surrounded by faceted terrain and TARs. The smooth surfaces of the yardangs are interpreted to be characteristic of the bedrock, while the faceted terrain is likely to be a secondary morphology created by the induration and subsequent scouring of depositional TAR networks. Portion of HiRISE image PSP_004216_1730. (b) Distinct complex TARs (black arrow) grade into complex terrain/bidirectional yardangs (white arrow) (Portion of HiRISE image ESP_017098_1745).

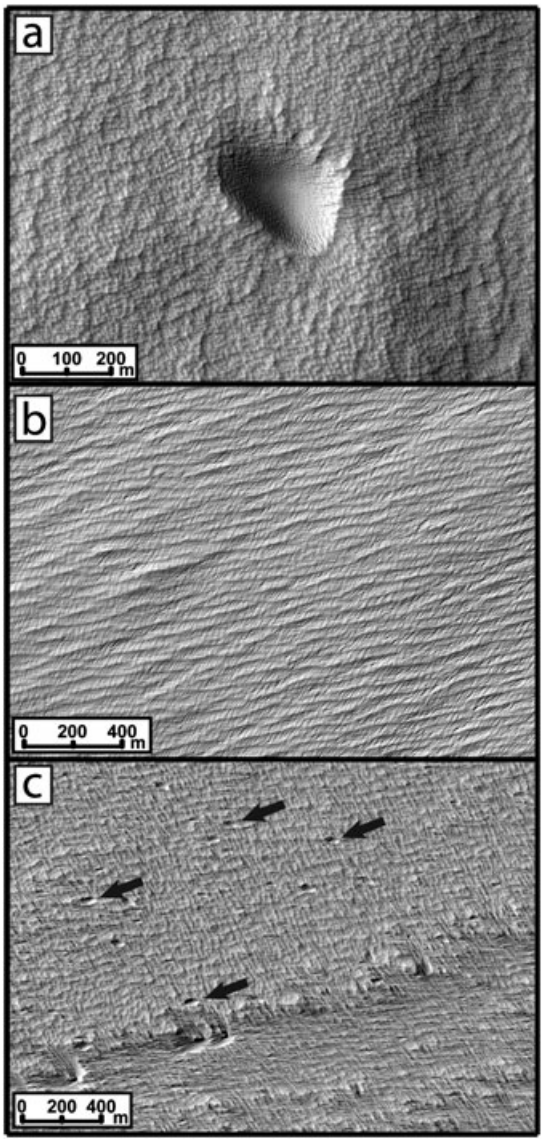

Figure 13. Possible end-member bedforms. (a) 'Network' faceted terrain with a similar pattern and wavelength to network dune fields elsewhere in the Medusae Fossae Formation (portion of HiRISE PSP_001446_1790). (b) 'Linear' faceted terrain with a similar pattern and wavelength to linear or transverse dune fields elsewhere (portion of HiRISE image PSP_008962_1785). (c) Due to the rough terrain, aeolian scours and notches (arrows) can form because of the complex flow of wind over the surface, eventually rendering the original TAR-covered surface difficult to recognize as an originally depositional landscape. Small craters could also initiate erosion (portion of HiRISE image PSP_010083_1775).

induration process which was able to strengthen them so that they no longer migrate under moderate wind velocities. On the basis of our observations, the induration process taking place in the MFF has allowed MFF TARs to survive long enough to become degraded and cratered, a somewhat rare occurrence on other parts of Mars. This suggests that either the mode of induration taking place in the MFF yields more resistant surfaces than elsewhere on Mars, or that the TARs formed and became indurated at an earlier time than aeolian bedforms (TARs and sand dunes) elsewhere on Mars.

The mode of induration of these deposits is as yet unknown, though there are several induration processes known or

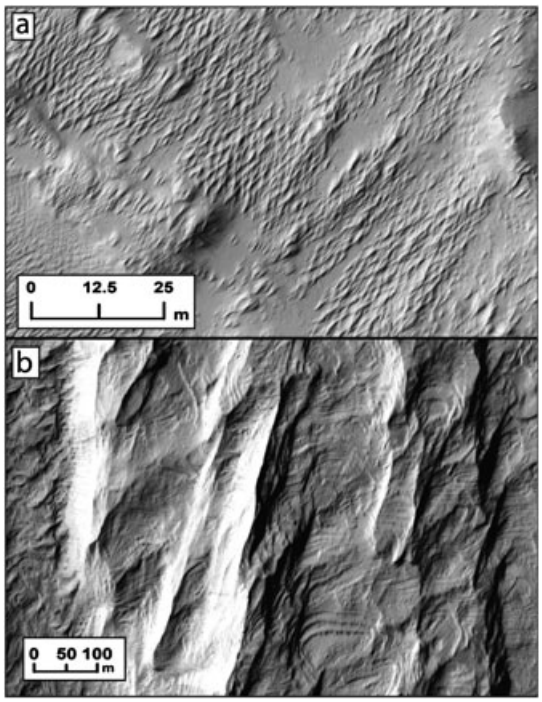

Figure 14. End-member terrains. a) Bidirectional yardangs, which could be formed from the erosion of indurated network TARs (portion of HiRISE image PSP_007763_1805). (b) Swirling, discontinuous layers in a yardang, possibly indicative of the variable dip of bedding typical of an aeolianite (portion of HiRISE image PSP_009464_1695).

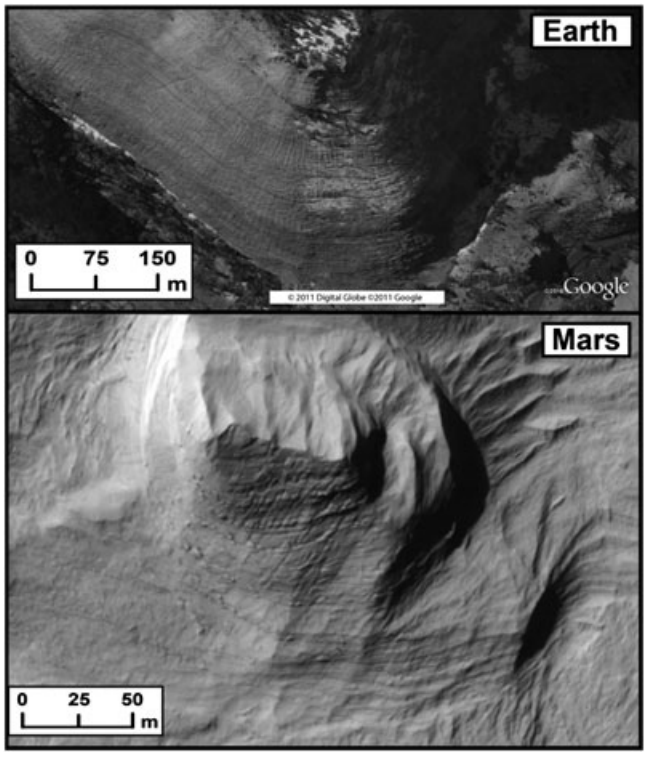

Figure 15. A comparison of (a) the Navajo Sandstone in Utah, USA with (b) an MFF yardang face on Mars. Note subtle layering and jointing in both cases. (a) Digital Globe image from Google Earth, image catalog number 101001000407DA02, taken 02/04/05, lat: 37.22 N, lon: 112.89 W. (b) Portion of HiRISE image ESP_017534_1690.

hypothesized to exist on Mars. The coarse-grained ripples studied by the Spirit Rover were described as covered in dust and having a crust (Sullivan *et al.*, 2008). Dust could inhibit movement of coarse-grained ripples because it is less easy to loft than slightly larger particle-sizes (Bagnold, 1941; Greeley and Iversen, 1985). Chemical cements such as calcrete, silcrete, alcrete, gypcrete, ferricrete, or sulfate compounds have been suggested as the means of induration at work in inverted terrain on Mars (Pain *et al.*, 2007). These types of cementing agents are commonly found in duricrusts in the tropical and arid zones of Earth (Desen and Peterson, 1992) and could also be a means of indurating the MFF TARs. It has been proposed that sedimentary silica could be important on Mars, weathering from the non-quartz portions of basaltic rocks or from volcanic glass (McLennan, 2003). Further orbital and surface exploration and analysis of the MFF is necessary to identify the most likely candidate induration processes and materials.

Whether they are long-wavelength ripples or transverse dunes, TARs are most likely composed of either sand-sized particles (0.062.5–2 mm) or coarse granules (2–4 mm) (Wentworth, 1922). The presence of yardangs suggests that the sand-sized or granule particles must be coherent and durable enough to abrade at least the yardang troughs. The presence of TARs thus implies that the MFF is made up of a significant portion of sand or granule particles. Large quantities of sand would suggest a proximal source for major components of the MFF, as sand cannot be transported as far from its source as dust can.

Conclusions

Numerous indurated and eroded transverse and networked aeolian ridges have been documented within the equatorial Medusae Fossae Formation. Cratered dunes and TARs are seldom seen elsewhere on Mars, an observation that we interpret to mean that these particular TAR-like bedforms in the MFF have been inactive for much longer than TARs and dunes found elsewhere. The presence of indurated and eroded bedforms in the MFF supports the hypothesis that the Medusae Fossae has undergone multiple cycles of erosion. This hypothesis suggests that a large part of the MFF in its present configuration is likely to be composed of secondary and tertiary deposits derived from erosion, reworking and redeposition of the MFF. This interpretation is consistent with the many ambiguous stratigraphic relationships found within the MFF that suggest erosion and reworking (Kerber and Head, 2010). This hypothesis is also consistent with the wide variety of deposit and feature morphologies present in the MFF and the tendency for one type of terrain to grade into another (for example, small changes in wind regime and particle availability could make the difference between a sea of network TARs, 'faceted' terrain, and bidirectional yardang terrain). In this context, the age of any particular region of the MFF would reflect only its particular stage in the recycling process, rather than its absolute age of emplacement. The young Amazonian crater age of the MFF (Scott and Tanaka, 1986; Greeley and Guest, 1987; Werner, 2006) is thus interpreted to be a crater retention age (Schultz and Lutz, 1988; Schultz, 2002; Kerber and Head, 2010) rather than a formation or original emplacement age. Evidence from MFF stratigraphic relationships with Hesperian-aged lava flows (Kerber and Head, 2010) suggest instead that the formation age of the MFF is at least as old as Hesperian (a period lasting between 3.5 Ga and 3.4 to 2.0 Ga; Hartmann and Neukum, 2001).

Fundamentally, the use of morphological and stratigraphic clues to determine the formation mechanism of the MFF depends on the assumption that these traits are related to the primary emplacement of the formation. For example, the presence of MFF material stratigraphically above a given lava surface implies that the MFF was deposited there after the lava cooled, but it does not necessarily guarantee that it was

deposited there by its primary emplacement mechanism (it may have been merely redistributed by the wind). Similarly, morphological features present in the deposit, including the appearance of jointing and layering, may provide important information about the original formation, emplacement and induration mechanisms for the MFF. However, our data suggest that such features could also have been created during subsequent modification of the deposit. We conclude that it is highly likely that much of the surface of the MFF as it is seen today does not reflect the conditions of its primary emplacement. The variety in degradational states observed in MFF TARs suggests that TAR formation, induration, and degradation is a significant and ongoing process within the formation.

Acknowledgments—LK gratefully acknowledges financial support provided by NASA Graduate Student Research Program (GSRP) grant NNX09AJ11H; JWH gratefully acknowledges financial support as part of the NASA/ESA participation in the Mars Express High-Resolution Stereo Camera Team under JPL Grant 1237163, and the Mars Data Analysis Program, MDAP Grant NNX09A146G. We also thank the two helpful anonymous reviewers who contributed to this manuscript, and JL Dickson and LM Garcia for technical assistance.

References

Bagnold R. 1941. *The Physics of Blown Sand and Desert Dunes*. Methuen: London.

Balme M, Berman DC, Bourke MC, Zimbelman JR. 2008. Transverse aeolian ridges (TARs) on Mars. *Geomorphology* **101**: 703–720.

Berman DC, Balme MR, Rafkin SCR, Zimbelman JR. 2011. Transverse aeolian ridges (TARs) on Mars II: distributions, orientations, and ages. *Icarus* **213**: 116–130. DOI: 10.1016/j.icarus.2011.02.014

Bosworth TO. 1922. *Geology and Paleontology of Northwest Peru*. Macmillan: London; 269–311.

Bourke MC, Edgett KS, Cantor BA. 2008. Recent aeolian dune change on Mars. *Geomorphology* **94**: 247–255.

Bourke MC, Wilson SA, Zimbelman JR. 2003. The variability of TARs in troughs on Mars. *Lunar and Planetary Science Conference* **35**: Abs. 2090.

Bradley BA, Sakimoto SEH, Frey H, Zimbelman JR. 2002. Medusae Fossae Formation: new perspectives from Mars Global Surveyor. *Journal of Geophysical Research* **107**: E8.

Breed CS, McCauley JF, Whitney MI. 1989. Wind erosion forms. In *Arid Zone Geomorphology*, Thomas DSG (ed). Belhaven Press: London; 284–307.

Bridges NT, Bourke MC, Colon CM, Diniega S, Geissler PE, Golombek MP, Hansen CJ, Mattson S, McEwen AS, Stantzos N. 2011. Planet-wide sand movement on Mars as documented by the HiRISE camera. *Lunar and Planetary Science Conference* **42**: Abs. 1215.

Bridges NT, Geissler PE, McEwen AS, Thomson BJ, Chuang FC, Herkenhoff KE, Keszthelyi LP, Martinez-Alonso S. 2007. Windy Mars: a dynamic planet as seen by the HiRISE camera. *Geophysical Research Letters* **34**: L23205. DOI: 10.1029/2007GL031445

Carter LM, Campbell BA, Watters TR, Phillips RJ, Putzig NE, Safaeinili A, Plaut JJ, Okubo CH, Egan AF, Seu R, Biccari D, Orosei R. 2009. Shallow radar (SHARAD) sounding observations of the Medusae Fossae formation, Mars. *Icarus* **199**: 295–302. DOI: 10.1016/j.icarus.2008.10.007

Desen T, Peterson J. 1992. Mapping the Australian duricrusts: can distribution be derived from terrain maps? *Australian Geographical Studies* **30**: 87–93.

Edgett KS, Malin MC. 2000. Examples of martian sandstone: indurated, lithified, and cratered eolian dunes in MGS MOC images. *Lunar and Plantery Science Conference* **31**: Abs. 1071.

Fenton LK. 2006. Dune migration and slip face advancement in the Rabe Crater dune field, Mars. *Geophysical Research Letters* **33**: L20201. DOI: 10.1029/2006GL027133

Fenton LK, Hayward RK. 2010. Southern high latitude dune fields on Mars: morphology, aeolian inactivity and climate change. *Geomorphology* **121**: 98–121.

Geissler PE, Stantzos NW, Bridges NT, The HiRISE Science Team. 2011. Shifting sands on Mars: 3 case studies. *Lunar and Planetary Science Conference* **42**: Abs. 2537.

Goudie AS. 2007. Mega-yardangs: a global analysis. *Geography Compass* **1**: 65–81.

Greeley R, Guest J. 1987. Geologic map of the eastern equatorial region of Mars. USGS Misc. Inv. Series Map I-1802-B, scale 1:15 M.

Greeley R, Iversen JD. 1985. *Wind as a geological process: on Earth, Mars, Venus and Titan*. Cambridge University Press: New York.

Greeley R, Lancaster N, Lee S, Thomas P. 1992. Martian aeolian processes, sediments, and features. In *Mars*, Kieffer HH, Jakosky BM, Snyder C, Matthews MS (eds). University of Arizona Press: Tucson; 730–766,

Hartmann WK, Neukum G. 2001. Cratering chronology and the evolution of Mars. *Space Science Reviews* **96**: 165–194.

Hayward RK, Mullins KF, Fenton LK, Hare TM, Titus TN, Bourke MC, Colaprete A, Christensen PR. 2007. Mars Global Digital Dune Database and initial science results. *Journal of Geophysical Research* **112**: E11007. DOI: 10.1029/2007JE002943

Head JW, Kreslavsky M. 2004. Medusae Fossae Formation: ice-rich airborne dust deposited during periods of high obliquity? *Lunar and Planetary Science Conference* **35**: Abs. 1635.

Hedin S. 1903. *Central Asia and Tibet*. Charles Scribner's Sons: New York; 608.

Hodgson RA. 1961. Regional study of jointing in Comb Ridge-Navajo Mountain Area, Arizona and Utah. *AAPG Bulletin* **45**. DOI: 10.1306/0BDA6278-16BD-11D7-8645000102C1865D

Hynek BM, Phillips RJ, Arvidson RE. 2003. Explosive volcanism in the Tharsis region: Global evidence in the martian geologic record. *Journal of Geophysical Research* **108**: E9.

Kerber L, Head JW. 2010. The age of the Medusae Fossae Formation: Evidence of Hesperian emplacement from crater morphology, stratigraphy, and ancient lava contacts. *Icarus* **206**: 669–684.

Kerber L, Head JW, Madeleine JB, Forget F, Wilson L. 2011. The dispersal of pyroclasts from Apollinaris Patera, Mars: Implications for the origin of the Medusae Fossae Formation. *Icarus* **216**: 212–220.

Kocurek G. 1991. Interpretation of ancient eolian sand dunes. *Annual Reviews of Earth and Planetary Science* **19**: 43–75.

Kreslavsky MA, Head JW. 2000. Kilometer-scale roughness of Mars: results from MOLA data analysis. *Journal of Geophysical Research* **105**: 26,711–26,.

Livingstone I, Warren A. 1996. *Aeolian Geomophology: an Introduction*. Addison Wesley Longman Limited: Singapore; 32–34.

Malin MC, Carr MH, Danielson GE, Davies ME, Hartmann WK, Ingersoll AP, James PB, Masursky H, McEwen AS, Soderblom LA, Thomas P, Veverka J, Caplinger MA, Ravine MA, Soulanille TA, Warren JL. 1998. Early views of the martian surface from the Mars Orbiter Camera on Mars Global Surveyor. *Science* **279**: 1681–1685.

Malin MC, Bell JF, Cantor BA, Caplinger MA, Calvin WM, Clancy RT, Edgett KS, Edwards L, Haberle RM, James PB, Lee SW, Ravine MA, Thomas PC, Wolff MJ. 2007. Context Camera investigation on board the Mars Reconnaissance Orbiter. *Journal of Geophysical Research* **112**: E05S04. DOI: 10.1029/2006JE002808

Malin MC, Edgett KS. 2000. Sedimentary rocks of early Mars. *Science* **290**: 1927–1937.

Mandt KE, de Silva S, Zimbelman JR, Crown DA. 2007. A synoptic approach to evaluating the origin of the Medusae Fossae Formation, Mars. *Lunar and Planetary Science Conference* **38**: Abs. 1823.

Mandt KE, de Silva SL, Zimbelman JR, Crown DA. 2008. Origin of the Medusae Fossae Formation, Mars: Insights from a synoptic approach. *Journal of Geophysical Research* **113**: E12011. DOI: 10.1029/2008JE003076

McCauley JF, Breed CS, El-Baz F, Whitney MI, Grolier MJ, Ward AW. 1979. Pitted and fluted rocks in the western desert of Egypt—Viking comparisons. *Journal of Geophysical Research* **84**: 8222–8232.

McCauley JF, Ward AW, Breed CS, Grolier MJ, Greeley R. 1977. Experimental modeling of wind erosion forms. *National Aeronautics and Space Administration Technical Memorandum X-3511*; 150–152.

McEwen AS, Eliason EM, Bergstrom JW, Bridges NT, Hansen CJ, Delamere WA, Grant JA, Gulick VC, Herkenhoff KE, Keszthelyi L, Kirk RL, Mellon MT, Squyres SW, Thomas N, Weitz CM. 2007. Mars Reconnaissance Orbiter's High Resolution Imaging Science Experiment (HiRISE). *Journal of Geophysical Research* **112**: E05S02. DOI: 10.1029/2005JE002605

McLennan SM. 2003. Sedimentary silica on Mars. *Geology* **31**: 315–318.

Neukum G, Jaumann R. 2004. HRSC: The High Resolution Stereo Camera on Mars Express. In Mars Express: the Scientific Payload. Wilson A (ed). ESA SP-1240; 17–35.

Pain CF, Clarke JDA, Thomas M. 2007. Inversion of relief on Mars. *Icarus* **190**: 478–491.

Sakimoto SEH, Frey HV, Garvin JB, Roark JH. 1999. Topography, roughness, layering, and slope properties of the Medusae Fossae Formation from Mars Orbiter Laser Altimeter (MOLA) and Mars Orbiter Camera (MOC) data. *Journal of Geophysical Research* **104**: 22,154–24,141.

Sayles RW. 1931. Bermuda during the ice age. *Proceedings of the American Academy of Arts and Sciences* **66**: 381–468.

Schultz PH. 2002. Uncovering Mars. *Lunar and Planetary Science Conference* **38**: Abs. 1790.

Schultz PH, Lutz AB. 1988. Polar wandering of Mars. *Icarus* **73**: 91–141.

Scott DH, Tanaka KL. 1982. Ignimbrites of Amazonis Planitia region of Mars. *Journal of Geophysical Research* **87**: 1179–1190.

Scott, DH, Tanaka KL. 1986. Geologic map of the western equatorial region of Mars. USGS Miscellaneous Investigations Series Map I-1802-A, scale 1:15 M.

Sharp RP. 1963. Wind ripples. *Journal of Geology* **71**: 617–636.

Silvestro S, Fenton LK, Vaz DA, Bridges NT, Ori GG. 2010. Ripple migration and dune activity on Mars: evidence for dynamic wind processes. *Geophysical Research Letters* **37**: L20203. DOI: 10.1029/2010GL044743

Squyres SW, Arvidson RE, Bell JF, Brückner J, Cabrol NA, Calvin W, Carr MH, Christensen PR, Clark BC, Crumpler L, Des Marais DJ, d'Uston C, Economou T, Farmer J, Farrand W, Folkner W, Golombek LM, Gorevan S, Grant JA, Greeley R, Grotzinger J, Haskin L, Herkenhoff KE, Hviid S, Johnson J, Klingelhöfer G, Knoll AH, Landis G, Lemmon M, Li R, Madsen MB, Malin MC, McLennan SM, McSween HY, Ming DW, Moersch J, Morris RV, Parker T, Rice JW, Richter L, Rieder R, Sims M, Smith M, Smith P, Soderblom LA, Sullivan R, Wänke H, Wdowiak T, Wolff M, Yen A. 2004. The Opportunity Rover's Athena science investigation at Meridiani Planum, Mars. *Science* **306**: 1698–1703.

Sullivan R, Arvidson R, Bell JF, Golombek M, Guinness E, Greeley R, Herkenhoff K, Johnson J, Squyres S, Thompson S, Whelley P, Wray J. 2008. Wind-driven particles mobility on Mars: insights from MER observations at 'El Dorado' and surroundings at Gusev Crater. *Lunar and Planetary Science Conference* **39**: Abs. 2092.

Tanaka KL. 2000. Dust and ice deposition in the martian geologic record. *Icarus* **144**: 254–266.

Thomas PC, Malin MC, Carr MH, Danielson GE, Davies ME, Hartmann WK, Ingersoll, AP, James PB, McEwen AS, Soderblom LA, Veverka J. 1999. Bright dunes on Mars. *Nature* **397**: 592–594.

Ward AW. 1979. Yardangs on Mars: evidence of recent wind erosion. *Journal of Geophysical Research* **84**: B14.

Ward AW, Greeley R. 1984. Evolution of the yardangs at Rogers Lake, California. *Geological Society of America Bulletin* **95**: 829–837.

Wentworth CK. 1922. A scale of grade and class terms for clastic sediments. *Journal of Geology* **30**: 377–392.

Werner SC. 2006. Major Aspects of the Chronostratigraphy and Geologic Evolutionary History of Mars. PhD dissertation, Fachbereich Geowissenschaften Freie Universität, Berlin. www.diss.fu-berlin.de/2006/33/indexe.html

Whitney MI. 1983. Eolian features shaped by aerodynamic and vorticity processes. In *Eolian Sediments and Processes*, Brookfield ME, Ahlbrandt TS (eds). Elsevier: Amsterdam; 223–245.

Whitney MI. 1985. Yardangs. *Journal of Geological Education* **33**: 93–96.

Wilson SA, Zimbelman JR. 2004. Latitude-dependent nature and physical characteristics of transverse aeolian ridges on Mars. *Journal of Geophysical Research* **109**: E10003. DOI:10.1029/2004JE002247

Zimbelman, JR. 2010. Transverse aeolian ridges on Mars: first results from HiRISE images. *Geomorphology* **121**: 22–29. DOI: 10.1016/j.geomorph.2009.05.012

Zimbelman JR, Griffin LJ. 2010. HiRISE images of yardangs and sinuous ridges in the lower member of the Medusae Fossae Formation, Mars. *Icarus* **205**: 198–210.

Zimbelman JR, Crown DA, Grant JA, Hooper DM. 1997. The Medusae Fossae Formation, Amazonis Planitia, Mars: evolution of proposed hypotheses of origin. *Lunar and Planetary Science Conference* **28**: Abs. 1482.

Zimbelman JR, Irwin RP, Williams SH, Bunch F, Valdez A, Stevens S. 2009. The rate of granule ripple movement on Earth and Mars. *Icarus* **203**: 71–76.